

Article

Influence of Soil Plug on the Seismic Response of Bucket Foundations in Liquefiable Seabed

Xue-Qian Qu ¹, Rui Wang ^{1,*} , Jian-Min Zhang ¹ and Ben He ²

¹ State Key Laboratory of Hydrosience and Engineering, Department of Hydraulic Engineering, Tsinghua University, Beijing 100084, China

² Power China Huadong Engineering Corporation Limited, Hangzhou 311122, China

* Correspondence: wangrui_05@mail.tsinghua.edu.cn

Abstract: The suction installation process for bucket foundations for offshore wind turbines (OWTs) can cause the formation of soil plug within the bucket, which can affect the seismic performance of the OWT. Therefore, it is important to evaluate the influence of soil plug on the seismic performance of OWT on bucket foundations. In this study, a comprehensive set of high-fidelity solid–fluid coupled dynamic numerical simulations are conducted to analyze the seismic response of bucket foundations with a focus on the influence of soil plug and its potential mitigation. The influence of different bucket models, seabed soil densities, seabed inclination and reinforcement types, as well as soil plug removal techniques, are investigated. The results clearly show that the existence of soil plug has a significant unfavorable influence on the seismic performance of OWT on bucket foundations, especially for wide bucket foundations in mildly inclined seabeds, and should be considered in seismic design. Reinforcement methods, such as the application of an inner compartments, outer wings and inner pile, can improve the seismic performance of OWT on bucket foundations, with the application of an inner compartment being the most effective. Soil plug removal can alleviate the negative influence of soil plug, and should be adopted when possible.

Keywords: offshore wind turbine; bucket foundation; liquefiable seabed; seismic response; soil plug



Citation: Qu, X.-Q.; Wang, R.; Zhang, J.-M.; He, B. Influence of Soil Plug on the Seismic Response of Bucket Foundations in Liquefiable Seabed. *J. Mar. Sci. Eng.* **2023**, *11*, 598. <https://doi.org/10.3390/jmse11030598>

Academic Editor: Dong-Sheng Jeng

Received: 8 February 2023

Revised: 8 March 2023

Accepted: 9 March 2023

Published: 11 March 2023



Copyright: © 2023 by the authors. Licensee MDPI, Basel, Switzerland. This article is an open access article distributed under the terms and conditions of the Creative Commons Attribution (CC BY) license (<https://creativecommons.org/licenses/by/4.0/>).

1. Introduction

Wind energy is one of the fastest growing renewable energy sources [1,2]. The safety of wind turbines is crucial to the stability of harnessing wind energy. Under seismic conditions, soil liquefaction may cause damage to wind turbine foundations, such as during the 1986 North Palm Springs earthquake and the 1992 Northridge earthquake in the United States [3,4], and the 2011 Tohoku earthquake in Japan [5]. Currently, an increasing number of offshore wind turbines (OWTs) are being planned and constructed in seismically active zones [6–9], with a notable proportion of them adopting the bucket foundation due to cost- and time-efficiency.

Cui et al. [10,11] and Meng et al. [12] conducted studies to investigate the horizontal and longitudinal dynamic interaction of a coupled soil–pile system. Compared with traditional monopile foundations, the influence of the interaction between the bucket and soil should also take into account the interaction between the bucket and both the outside- and inside-bucket soil. In addition, bucket foundations can be more susceptible to liquefaction-induced seismic damage due to their shallow burial depth [13], especially in mildly inclined seabeds often encountered in offshore environments [14–16]. Additionally, the suction installation process for bucket foundations could lead to the formation of soil plug within the bucket that is higher than seabed, reducing the installation depth of the foundation [17–22], which could affect the interaction between the bucket and inside-bucket soil and further its seismic performance.

With the rapid application of bucket foundations for OWT, numerous studies have focused on the seismic response of bucket foundations. Yu et al. [23], Wang et al. [24],

Olalo et al. [25], Wang et al. [26], Wang et al. [27], Li et al. [28] and Zayed et al. [29] conducted studies to investigate the factors influencing the seismic response of bucket foundations through centrifuge shaking table tests. Asheghabadi et al. [30], Gao et al. [31], Gao et al. [13], Wang et al. [32] and Zayed et al. [29] studied the seismic response of bucket foundations in liquefiable seabeds via numerical analysis, focusing on the influence of bucket foundations' depth-to-diameter ratio, sand density, soil permeability and earthquake magnitudes. Esfeh et al. [33] and Ueda et al. [34] found that soil liquefaction may lead to a significant permanent tilt of bucket foundations under seismic load. Kourkoulis et al. [35] and Zhang et al. [36] analyzed the influence of soil–bucket dynamic interaction and interface properties on the seismic response of bucket foundation. Eslami et al. [37] compared the seismic response of OWT on monopiles and suction bucket foundations, and found that the geometric shape of the foundation imposes a complex influence. Qu et al. [16] revealed the nonnegligible effect of mild seabed rotation on the seismic performance of OWT on suction buckets within liquefiable soils. Liu et al. [38] studied the soil plug effect on the vertical dynamic response of piles, but there have yet to be studies on the influence of soil plug for the seismic performance of suction bucket-based OWTs.

To improve the static and dynamic stability of bucket foundations, various forms of reinforcement have been proposed, including arranging inner compartments within the bucket and wings outside the bucket and installing a pile within the bucket [39–44]. In addition, some novel types of composite bucket foundations have also been proposed, e.g., mat foundation with buckets [45–47]. To alleviate the undesired influence of the soil plug, Chen et al. [48], An et al. [49], He et al. [50] and Wang [22] proposed methods to limit or remove the soil plug formed during suction bucket installation. However, the effects of these reinforcement and soil plug removal techniques on improving the seismic performance of bucket foundations have yet to be comprehensively investigated.

During the installation of the suction bucket, the inside-bucket soil is disturbed, and a soil plug is often formed, which is known to be unfavorable for the stability of the foundation. This study aims to use a high fidelity soil constitutive model and numerical simulation method to evaluate the influence of soil plug on the seismic performance of OWT bucket foundations in both horizontal and inclined liquefiable seabeds, which has yet to be reported. The effectiveness of various reinforcement and soil plug removal techniques on improving the seismic performance of OWT bucket foundations that suffer from the formation of soil plug is also assessed. The details of the numerical analysis method are provided in Section 2. The influence of soil plug on the seismic response of bucket foundations is analyzed in Section 3. The effects of different reinforcement methods and the removal of soil plug on bucket foundations' seismic performance are discussed in detail in Sections 4 and 5, respectively.

2. Numerical Method

2.1. The OWT Model

In this study, two basic bucket foundation models with the same amount of steel usage were adopted. For the Wide Bucket Foundation (WBF) model, the bucket foundation had a diameter of 20 m and a height of 10 m. For the Deep Bucket Foundation (DBF) model, the bucket foundation had a diameter of 13 m and a height of 19.83 m. The wall thickness of the buckets was set to be 0.04 m. The remaining geometric parameters of the two bucket models were the same. The tower of the OWT was 80 m high and 5 m in diameter. The superstructure of the OWT was 250 t in mass (including generator, nacelle, rotor blade, etc.). The bucket used steel with a density of $7.9 \times 10^3 \text{ kg/m}^3$, Poisson's ratio of 0.3 and Young's modulus of 210 GPa.

Six reinforced bucket foundation models were also constructed based on the two basic models to analyze the effect of different reinforcement types on seismic performance. The reinforcement types considered in this study included inner-compartments within the bucket, outer-wings outside the bucket and a combination of pile with bucket. The geometric and reinforcement types of all eight bucket foundation models are listed in

Table 1, including the Deep Bucket Foundation (DBF), Deep Inner-Compartment Bucket Foundation (DBF-C), Deep Pile-Bucket Foundation (DBF-P), Deep Outer-Wings Bucket Foundation (DBF-W), Wide Bucket Foundation (WBF), Wide Inner-Compartment Bucket Foundation (WBF-C), Wide Pile-Bucket Foundation (WBF-P) and Wide Outer-Wings Bucket Foundation (WBF-W). Figure 1 visually depicts these eight models. Similar to the design of the two basic models, the reinforcement for the deep and wide models also had the same amount of steel usage for fair comparison.

Table 1. Geometry and reinforcement type for the bucket foundation models.

Model ID	Bucket Diameter	Bucket Height	Reinforcement Type
Model 1 (DBF)	13	19.83	Single Bucket
Model 2 (DBF-C)	13	19.83	Inner-Compartment Bucket
Model 3 (DBF-P)	13	19.83	Pile-Bucket
Model 4 (DBF-W)	13	19.83	Outer-Wing Bucket
Model 5 (WBF)	20	10	Single Bucket
Model 6 (WBF-C)	20	10	Inner-Compartment Bucket
Model 7 (WBF-P)	20	10	Pile-Bucket
Model 8 (WBF-W)	20	10	Outer-Wing Bucket

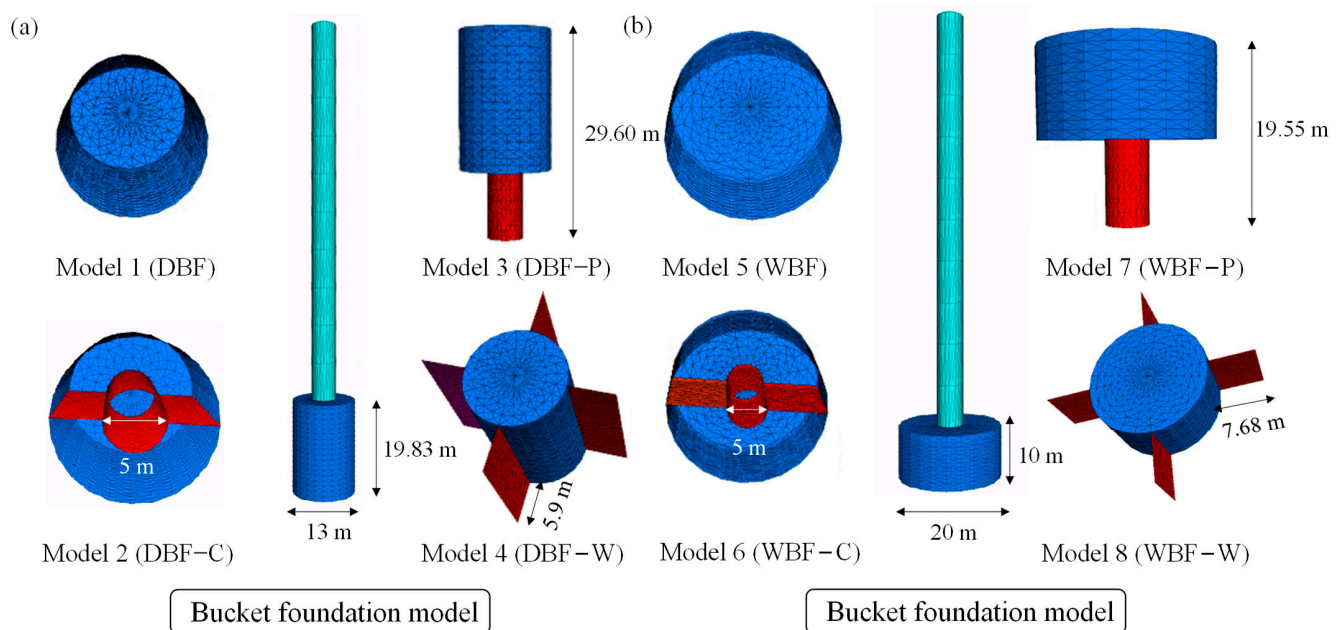


Figure 1. Bucket foundation model: (a) deep bucket foundation; (b) wide bucket foundation.

2.2. Seabed Soil Specification

In this study, dynamic solid–fluid coupled analysis using a plasticity constitutive model for seabed soil was conducted using the finite difference code FLAC3D [51]. The finite difference software FLAC3D is a widely used geotechnical engineering numerical analysis software [51]. FLAC3D is based on the explicit Lagrangian finite difference algorithm. The nature of the algorithm makes it robust for the large deformation of the computational grid, which is very suitable for the calculation of soil liquefaction-related problems involving large deformation and strong nonlinearity. This approach has been validated by Qu et al. [52]. The unified plasticity model for the large post-liquefaction shear deformation of sand (CycLiq) was developed by the authors in Wang et al. [53], and is used in this study to model the dynamic behavior of seabed soil. This unique model can simulate the mechanical behavior of sand in different states from pre- to post-liquefaction under monotonic and cyclic loading. The model has been implemented in FLAC3D [54], and has been successfully applied to various geotechnical earthquake

engineering problems, including soil–pile interaction, quay wall analysis, underground structure analysis, etc. [55–60]. The 14 model parameters used in this study are shown in Table 2, which contains the elastic modulus constants of G_0 and κ , the plastic modulus parameter of h , the critical state parameters of M , λ_c , e_0 and ξ , the state parameter of n^p and n^d , the reversible dilatancy parameters of $d_{re,1}$ and $d_{re,2}$ and the irreversible dilatancy parameters of d_{ir} , α and $\gamma_{d,r}$. The parameters used in this study are within reasonable ranges documented by Wang et al. [53] and Zou et al. [54]. The simulation results for a typical undrained cyclic torsional shear test of the sand with a void ratio of 0.65 using the constitutive model and designated parameters are shown in Figure 2a,b, which is representative of the typical cyclic liquefaction behavior of sand.

Table 2. Constitutive model parameter values used in this study.

G_0	κ	h	$d_{re,1}$	$d_{re,2}$	d_{ir}	α	$\gamma_{d,r}$	n^p	n^d	M	λ_c	e_0	ξ
200	0.006	1.7	0.45	30	0.6	40	0.05	1.1	8.0	1.3	0.023	0.837	0.7

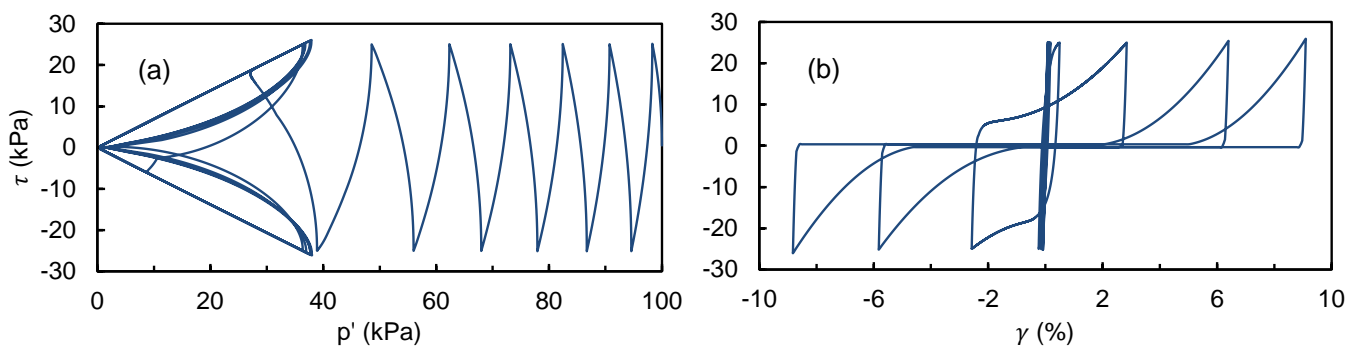


Figure 2. Simulation results for a typical undrained cyclic torsional shear test on sand with void ratio of 0.65: (a) effective stress path; (b) stress–strain relationship.

The hypothetical liquefiable sand has a maximum dry density of $1.70 \times 10^3 \text{ kg/m}^3$, a minimum dry density of $1.41 \times 10^3 \text{ kg/m}^3$ and a specific gravity of 2.65. Two different relative densities were considered in this study, including 50% and 80%, to check the consistency for the findings from the relatively loose and dense sand. The 50% relative density simulations were used as benchmark. The basic properties of the standard sand used in this study are listed in Table 3. Many offshore wind turbines are located in mildly inclined seabeds, such as the Rudong offshore wind turbine in Jiangsu, China, where the seabed inclination of the wind turbine is 0.68° . Both horizontal and mildly inclined seabeds are considered, with the slope of the inclined seabed analyzed in this paper being 0.85° (same as Qu et al. [16]).

Table 3. Basic properties of the standard sand in this study.

	Soil Outside the Bucket			Soil Inside the Bucket		
	Dry Density ρ_d (kg/m ³)	Permeability Coefficient k (cm/s)	Void Ratio e	Dry Density ρ_d (kg/m ³)	Permeability Coefficient k (cm/s)	Void Ratio e
Soil 1	1.54×10^3	1.5×10^{-2}	0.717	1.49×10^3	3×10^{-2}	0.782
Soil 2	1.64×10^3	5.0×10^{-3}	0.620	1.58×10^3	1.0×10^{-2}	0.677

To model the influence of soil plug, the height of the soil plug needs to be determined, along with the soil density and permeability within the bucket, both of which are affected by the formation of the soil plug. The height of the soil plug, in practice, is generally observed to be 30–50 cm [61,62], moreover the soil plug inside the suction bucket foundation of the

GORM oil field installed in sand was reported to have reached 3 m [17,49]. Based on these typical values, the height of the soil plug in the wide bucket foundation was set at 0.36 m, while the height of the soil plug in the deep bucket foundation was set at 0.7 m in this study. The soil density within the two bucket models (DBF and WBF) were therefore the same, but less than that of the outside soil, under the assumption of mass conservation during installation. For the case of an outside soil of 50% relative density, this means that the inside-bucket soil is at 30% relative density, whereas it is 62.4% for the 80% relative density case. In terms of permeability, Tran et al. [63] found that the permeability coefficients of inside soil can be twice that of outside soil due to the loosening of soil during suction installation. Therefore, the ratio of permeability coefficient of soil inside and outside the bucket was set to 2:1. Liu et al. [64] and Zhu et al. [57] tested the permeability coefficient of Fujian sand by constant head tests. The permeability coefficient of sand was adopted within the range of these previous tests in this paper, as shown in Table 3. Regarding the simulations for the effect of soil plug removal, the excess height of the soil plug was removed, while retaining the reduced density and increased permeability of the inside bucket soil.

2.3. Numerical Simulation Program

In this study, a total of 44 numerical simulations were conducted to account for the different bucket models, reinforcement types, seabed soil densities, seabed rotation and soil plug existence, and are listed in Table 4. Simulations 1–4 and 5–8 analyze the influence of soil plug on seismic response in horizontal and mildly inclined seabeds of 50% relative density, respectively. These seabed soil simulations were repeated for a dense seabed soil setting (80% relative density) in simulations 9–16. The influence of different reinforcement types was analyzed in simulations 17–28, for both horizontal and inclined loose seabeds with soil plug. Simulations 29–44 assessed the effect of reinforcement type on soil plug removal.

Table 4. Numerical simulations conducted in this study.

Simulation Number	Seabed Rotation	Relative Density of Inside-Bucket Soil	Relative Density of Outside-Bucket Soil	Soil Plug	Bucket Model
1	Horizontal	50%	50%	No	1 (DBF)
2	Horizontal	30%	50%	0.7 m	1 (DBF)
3	Horizontal	50%	50%	No	5 (WBF)
4	Horizontal	30%	50%	0.36 m	5 (WBF)
5	Inclined	50%	50%	No	1 (DBF)
6	Inclined	30%	50%	0.7 m	1 (DBF)
7	Inclined	50%	50%	No	5 (WBF)
8	Inclined	30%	50%	0.36 m	5 (WBF)
9	Horizontal	80%	80%	No	1 (DBF)
10	Horizontal	62.4%	80%	0.7 m	1 (DBF)
11	Horizontal	80%	80%	No	5 (WBF)
12	Horizontal	62.4%	80%	0.36 m	5 (WBF)
13	Inclined	80%	80%	No	1 (DBF)
14	Inclined	62.4%	80%	0.7 m	1 (DBF)
15	Inclined	80%	80%	No	5 (WBF)
16	Inclined	62.4%	80%	0.36 m	5 (WBF)
17	Horizontal	30%	50%	0.7 m	2 (DBF-C)
18	Horizontal	30%	50%	0.7 m	3 (DBF-P)
19	Horizontal	30%	50%	0.7 m	4 (DBF-W)
20	Horizontal	30%	50%	0.36 m	6 (WBF-C)
21	Horizontal	30%	50%	0.36 m	7 (WBF-P)
22	Horizontal	30%	50%	0.36 m	8 (WBF-W)
23	Inclined	30%	50%	0.7 m	2 (DBF-C)
24	Inclined	30%	50%	0.7 m	3 (DBF-P)

Table 4. Cont.

Simulation Number	Seabed Rotation	Relative Density of Inside-Bucket Soil	Relative Density of Outside-Bucket Soil	Soil Plug	Bucket Model
25	Inclined	30%	50%	0.7 m	4 (DBF-W)
26	Inclined	30%	50%	0.36 m	6 (WBF-C)
27	Inclined	30%	50%	0.36 m	7 (WBF-P)
28	Inclined	30%	50%	0.36 m	8 (WBF-W)
29	Horizontal	30%	50%	Removed	1 (DBF)
30	Horizontal	30%	50%	Removed	2 (DBF-C)
31	Horizontal	30%	50%	Removed	3 (DBF-P)
32	Horizontal	30%	50%	Removed	4 (DBF-W)
33	Horizontal	30%	50%	Removed	5 (WBF)
34	Horizontal	30%	50%	Removed	6 (WBF-C)
35	Horizontal	30%	50%	Removed	7 (WBF-P)
36	Horizontal	30%	50%	Removed	8 (WBF-W)
37	Inclined	30%	50%	Removed	1 (DBF)
38	Inclined	30%	50%	Removed	2 (DBF-C)
39	Inclined	30%	50%	Removed	3 (DBF-P)
40	Inclined	30%	50%	Removed	4 (DBF-W)
41	Inclined	30%	50%	Removed	5 (WBF)
42	Inclined	30%	50%	Removed	6 (WBF-C)
43	Inclined	30%	50%	Removed	7 (WBF-P)
44	Inclined	30%	50%	Removed	8 (WBF-W)

The numerical model of the simulation for the deep bucket foundation is shown in Figure 3. In FLAC3D, solid–fluid coupling is achieved by solving both the equilibrium of the solid and fluid phases sequentially [51]. The bucket foundation was simulated using liner structural elements, which can consider the interaction between bucket and soil. The turbine tower was simulated using shell elements, with a height of 80 m and a diameter of 5 m. The bucket foundation and turbine tower had a density of $7.9 \times 10^3 \text{ kg/m}^3$, Poisson's ratio of 0.3 and Young's modulus of 210 GPa. The superstructure of OWT was modeled as a circular shell element, with a thickness of 0.4 m, a diameter of 5 m and a density of $31.85 \times 10^3 \text{ kg/m}^3$. The seabed soil model was 150 m long, 150 m wide and 40 m high to limit the influence of boundary effect [65], and the free field condition under horizontal shaking was achieved using the tied boundary, where the nodes of the same height on the left and right boundaries of the model were forced to follow the same motion. Minimal Rayleigh damping was used for seabed soil, considering that the constitutive model inherently included damping. A free drainage condition was applied at the soil surface. Regardless of the influence of the water pressure above the soil surface, which was the same on both sides of the bucket, the pore pressure of the soil surface outside the bucket was set to the same water pressure value as the height of the soil plug, and the pore pressure of the soil surface outside the bucket was set to 0 for the condition without the soil plug. The left, right and bottom boundaries of the model were undrained. Liner structural elements simulated the relative sliding and separation between the soil and bucket, which adopted the Mohr–Coulomb model. The normal coupling spring stiffness k_n and shear coupling spring stiffness k_s were set according to the stiffest neighboring zone [51]. The strength parameters were taken as $c = 0 \text{ kPa}$ and friction angle $\varphi = 20^\circ$ following existing studies [37,51,66,67]. Horizontal seismic input was applied to the base of the model. Referring to several typical OWT projects in China, including the Jiangsu Dafeng 300MW offshore wind farm with design peak ground acceleration of 0.2 g (0.3 g) [68–70], the input motion with peak acceleration of 0.23 g was used in this study. The input motion was scaled from the 1966 Parkfield ground motion, as shown in Figure 4. It should be noted that different input motions will cause different quantitative results, but do not affect the qualitative influence of the soil plug, which is the main focus of this study.

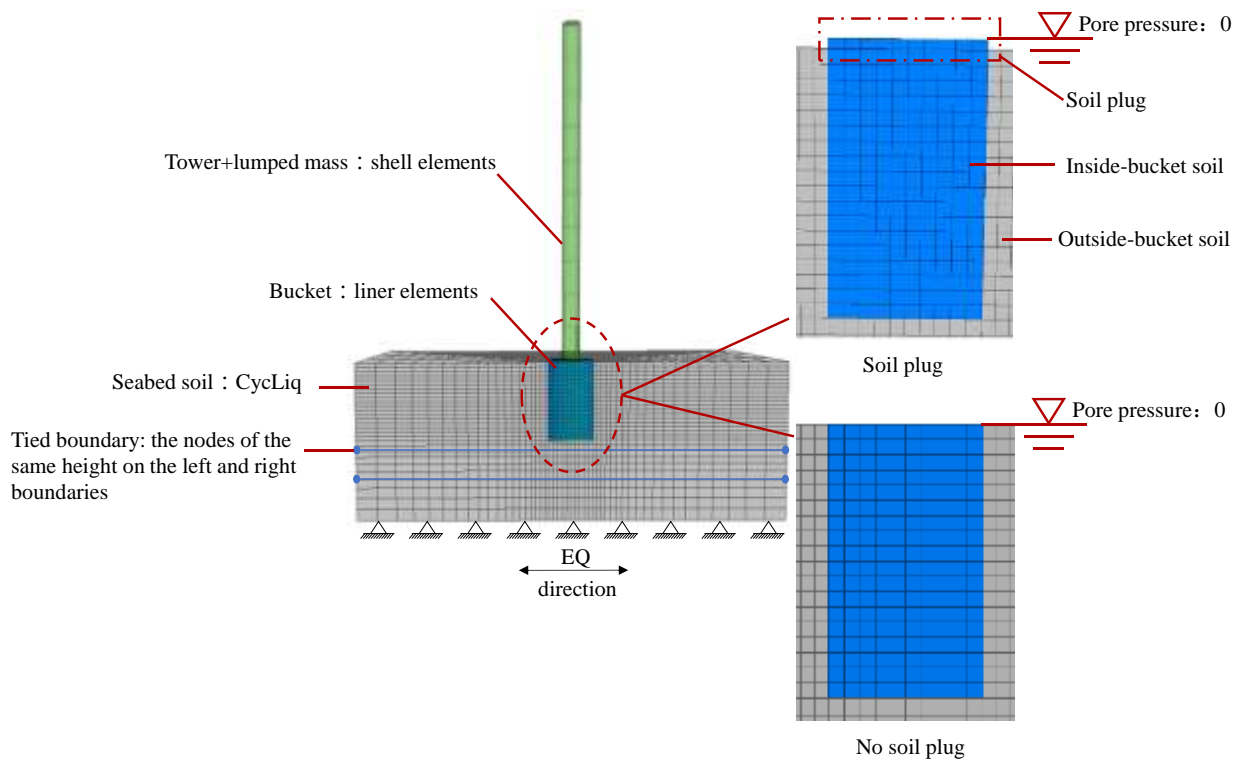


Figure 3. Numerical analysis model for the deep bucket foundation case in FLAC3D.

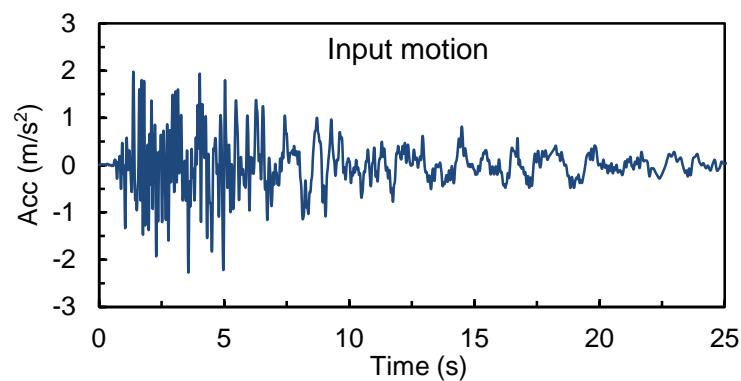


Figure 4. The acceleration time history of input motion.

3. Influence of Soil Plug on OWT Bucket Foundation Response

By comparing the results of bucket foundation response analysis with and without soil plug (simulations one–four and five–eight in Table 4), the influence of the soil plug can be identified. For the wide bucket foundation (WBF), the acceleration time histories of seabed soil and OWT superstructure at different positions in 50% relative density inclined liquefiable seabeds with and without soil plug are shown in Figure 5 (simulations seven and eight). The soil plug had almost no influence on the acceleration of the far field soil, as expected. Attenuation of acceleration was observed in the far field soil due to the softening and liquefaction of soil, especially near the seabed surface, as shown in Figure 5a–c. The confining effect of the bucket skirt led to the amplification of acceleration in the inside-bucket soil, which was consistent with the centrifuge test observations in Qu et al. [16]. Compared with the case without soil plug, the presence of soil plug caused slight amplification of acceleration for inside-bucket soil, bucket and turbine, as shown in Figure 5d–f. The peak accelerations of the bucket and turbine were 1.28 m/s² and 0.99 m/s² when there was soil plug in the bucket, respectively, which were 1.22 and 1.16 times that of

the case without soil plug, as shown in Figure 5e,f. This was mainly caused by the raised height of the structure, as the soil plug prevents the bucket from full penetration.

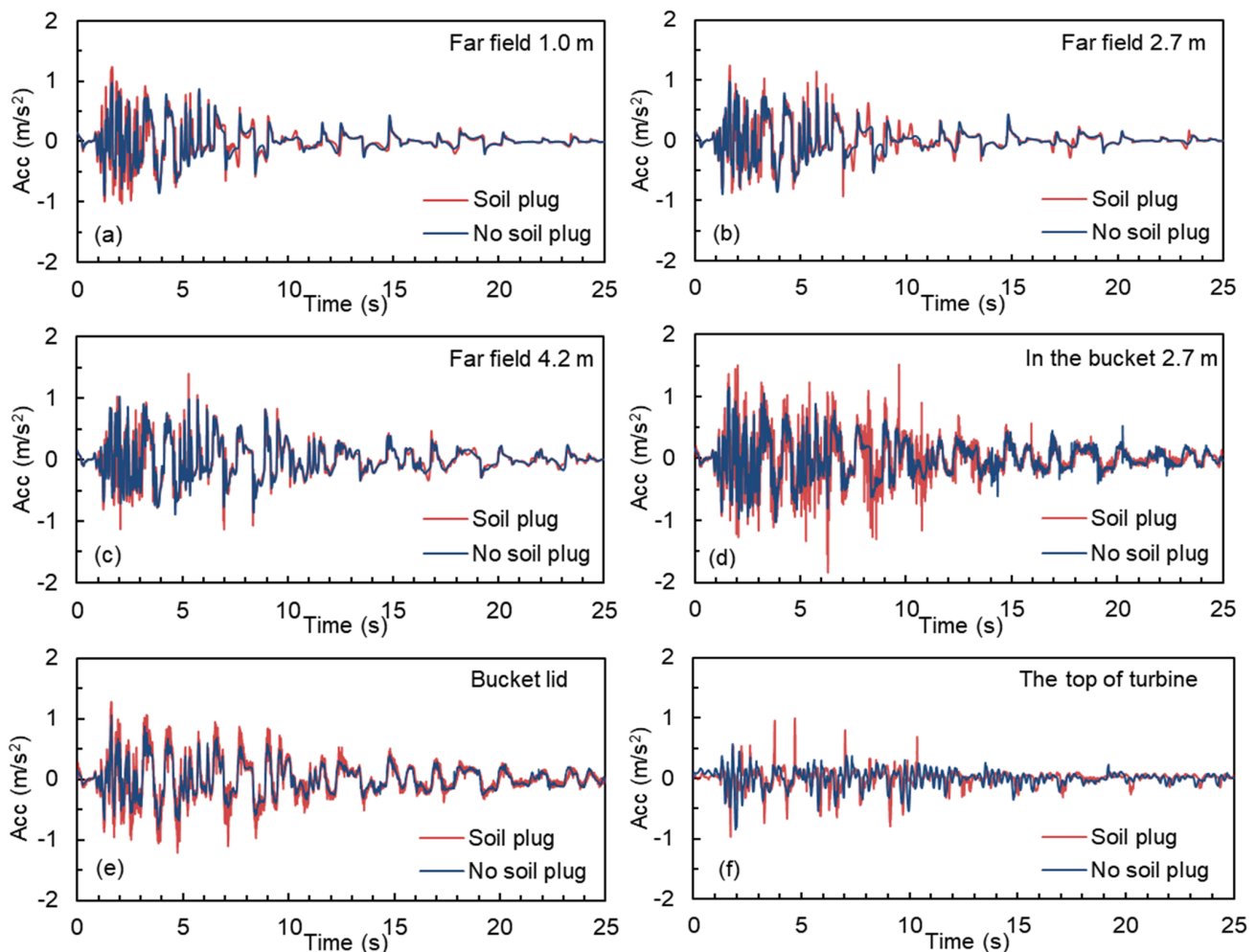


Figure 5. Acceleration time histories for seabed soil and turbine (WBF) with and without soil plug in 50% relative density inclined liquefiable seabeds: (a) far field seabed soil at 1.0 m depth; (b) far field seabed soil at 2.7 m depth; (c) far field seabed soil at 4.2 m depth; (d) seabed soil in the bucket at 2.7 m depth; (e) bucket lid; (f) top of OWT turbine.

For the wide bucket foundation, the excess pore pressure time histories of seabed soil at different positions in simulations seven and eight are shown in Figure 6. Soil liquefaction was determined when the excess pore pressure was equal to the initial vertical effective stress. The initial vertical effective stress of the ground soil inside the bucket was higher compared with the free field due to the weight of the superstructure of OWT, and liquefaction should be determined based on the stress state considering such influence. The results show that the far field seabed soil was liquefied at 2.0 m depth, which was not influenced by the soil plug (Figure 6a). For near field, a stronger fluctuation in excess pore pressure was observed due to the interaction between bucket, soil and liquefaction was also reached at 2.0 m depth (Figure 6b). Within the bucket, greater excess pore pressure was generated due to the high initial effective stress caused by the self-weight of the superstructure of OWT, compared with that of near field and far field soil at the same depth, and was far from achieving liquefaction (Figure 6c). The existence of the soil plug significantly increased the accumulation of excess pore pressure in the soil inside and under the bucket (Figure 6c,d), which was associated with the increased structure response.

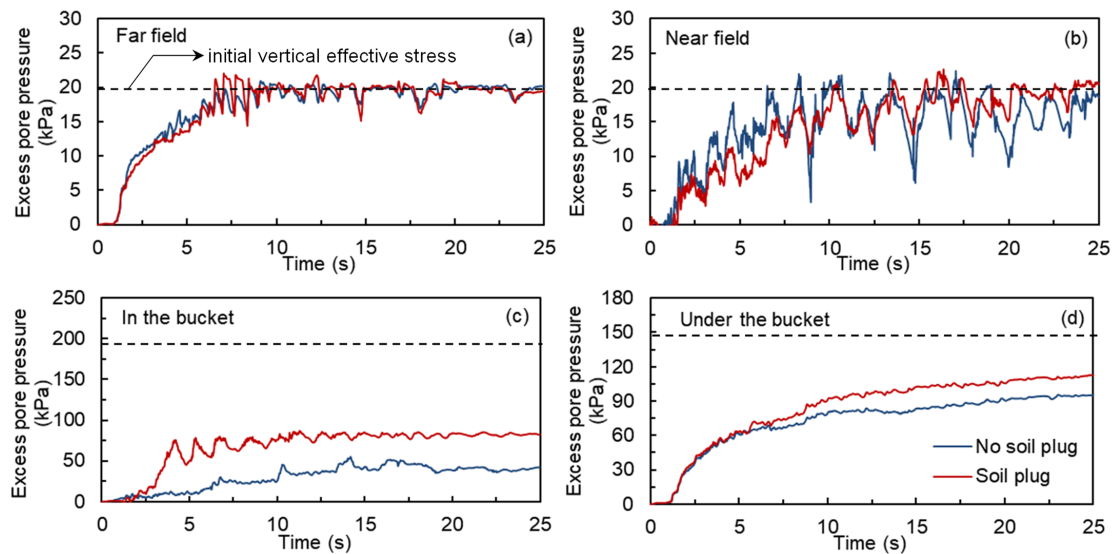


Figure 6. Excess pore pressure time histories of seabed soil for simulations with and without soil plug in 50% relative density inclined liquefiable seabeds: (a) far field seabed soil at 2.0 m depth; (b) near field seabed soil at 2.0 m depth; (c) seabed soil in the bucket at 2.0 m depth; (d) seabed soil under the bucket at 12 m depth.

More directly related to the seismic performance of the bucket foundation was its seabed displacement and rotation. The influence of soil plug on horizontal displacement time histories at the top of the bucket foundation for DBF and WBF in horizontal and inclined seabeds are shown in Figure 7 (simulations one–eight), where H represents horizontal ground and I represents inclined ground. The existence of soil plug led to an increase in the maximum horizontal displacement of bucket foundation in horizontal and inclined ground. In horizontal seabed, a slight increase in peak displacement was observed with soil plug, with almost no residual displacement. In inclined ground, an accumulation of horizontal displacement was observed, and the existence of soil plug significantly increased the residual horizontal displacement.

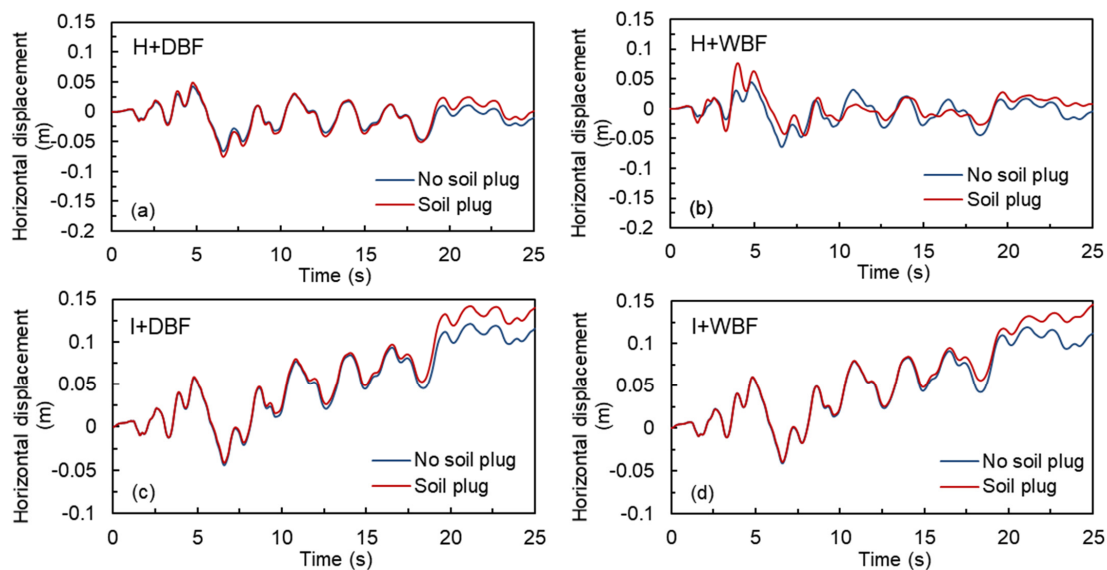


Figure 7. The horizontal displacement time histories at the top of the bucket foundations in 50% relative density liquefiable seabed: (a) deep bucket foundation (DBF) in horizontal liquefiable seabed; (b) wide bucket foundation (WBF) in horizontal liquefiable seabed; (c) deep bucket foundation (DBF) in inclined liquefiable seabed; (d) wide bucket foundation (WBF) in inclined liquefiable seabed. H refers to horizontal seabed and I refers to inclined seabed.

For a more straightforward comparison of the influence of soil plug on bucket displacement, Figure 8 plots the maximum horizontal displacement in liquefiable seabed for the scenarios (simulations one–eight). For the deep bucket foundation, the maximum horizontal displacement of the bucket foundation increased by 13.6% in the horizontal seabed and by 17.4% in the inclined seabed due to the existence of the soil plug. For the wide foundation, the maximum horizontal displacement of the bucket foundation increased by 18.8% in the horizontal seabed and by 22.7% in the inclined seabed due to the existence of the soil plug. Clearly, the soil plug imposed an undesired influence on the seismic performance of the bucket foundation, which was stronger for the shallower wide foundation. The residual horizontal displacement of the WBF in inclined ground was 0.146 m, which is within the failure horizontal displacement criterion of 3–6% bucket diameter [71].

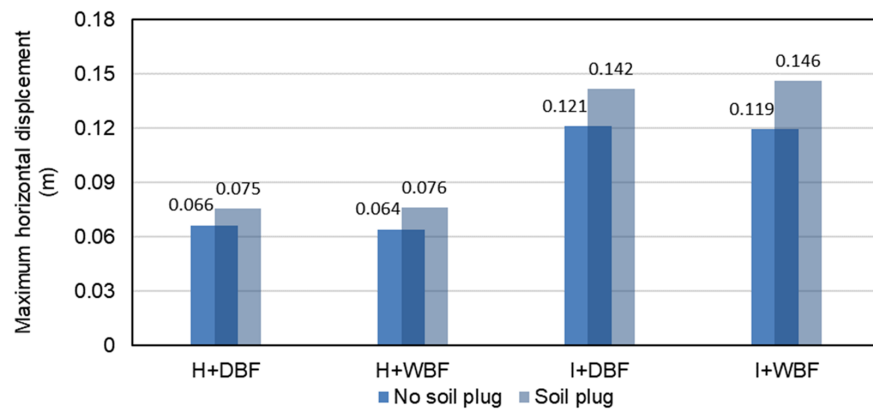


Figure 8. The maximum horizontal displacement of bucket foundations in 50% relative density liquefiable seabeds.

The bucket foundation rotation time histories in liquefiable seabeds (simulations one–eight) are shown in Figure 9. In horizontal seabed, soil plug caused a major amplification in the rotation of WBF, whereas in inclined seabed, it amplified the residual rotation of WBF and DBF. In particular, in inclined seabed, soil plug caused the maximum rotation of the WBF to reach 1.51°, while it also increased the rotation of the DBF from 0.235° to 0.275°, exceeding the failure rotation criterion of 0.25° [72].

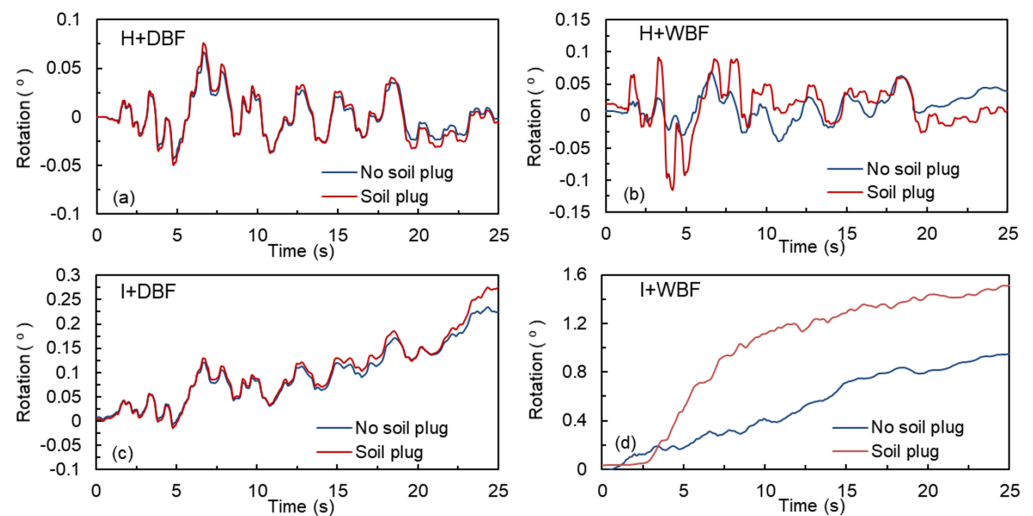


Figure 9. The rotation time histories of bucket foundations in 50% relative density liquefiable seabeds: (a) deep bucket foundation (DBF) in horizontal liquefiable seabeds; (b) wide bucket foundation (WBF) in horizontal liquefiable seabeds; (c) deep bucket foundation (DBF) in inclined liquefiable seabeds; (d) wide bucket foundation (WBF) in inclined liquefiable seabeds. H refers to horizontal seabeds and I refers to inclined seabeds.

The maximum rotations of WBF and DBF in horizontal ground and inclined ground with and without soil plug are directly compared in Figure 10. The maximum rotation of DBF increased by 13.4% in horizontal ground and by 17.0% in inclined ground with soil plug, while the maximum rotation of WBF increased by 3.6% in horizontal ground and by 58.8% in inclined ground with soil plug. In general, the WBF was more significantly impacted by the soil plug. These results suggest that it is important to consider the potential undesired influence of soil plug in the seismic design of OWT on bucket foundations, especially in inclined seabeds.

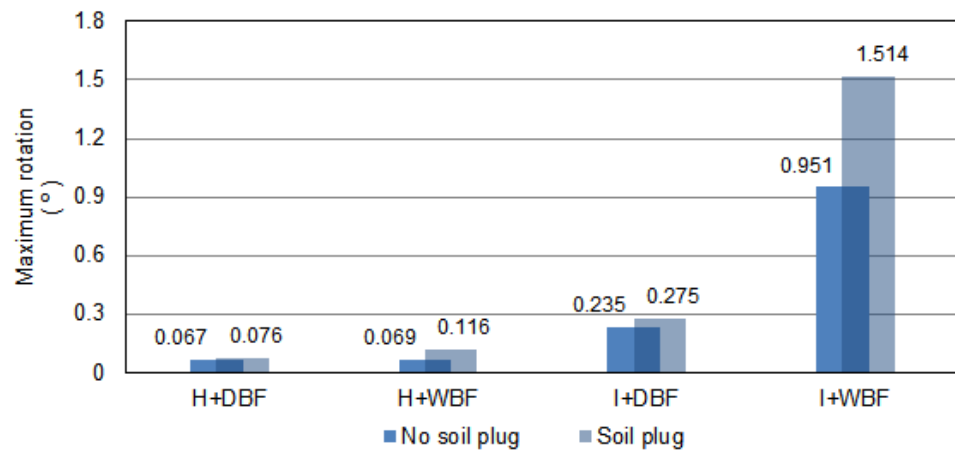


Figure 10. The maximum rotation of bucket foundations in 50% relative density liquefiable seabeds.

Compared with the residual horizontal displacement in the shaking direction (X) of 0.146 m for the wide bucket foundation, the horizontal residual displacement in the direction perpendicular to shaking (Y) was only 0.0049 m (as shown in Figure 11), which is negligible. Therefore, only the horizontal response in the X direction is analyzed from hereon.

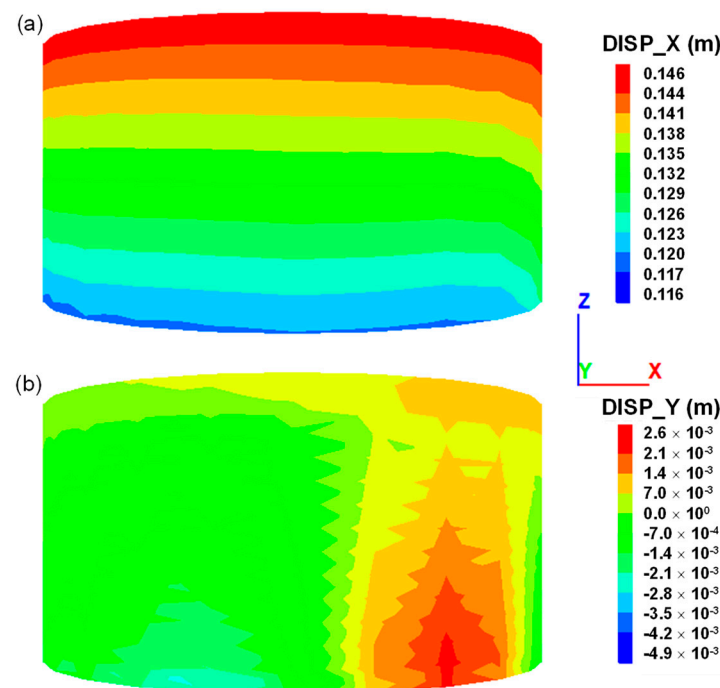


Figure 11. The residual horizontal displacement of bucket: (a) shaking direction; (b) the direction perpendicular to shaking.

The settlement time histories at the left and right corner points of the wide bucket foundation (WBF) in inclined liquefiable seabeds are shown in Figure 12. The existence of soil plug increased the nonuniform settlement of bucket, where a slight increase in the peak settlement in the right point of bucket was observed.

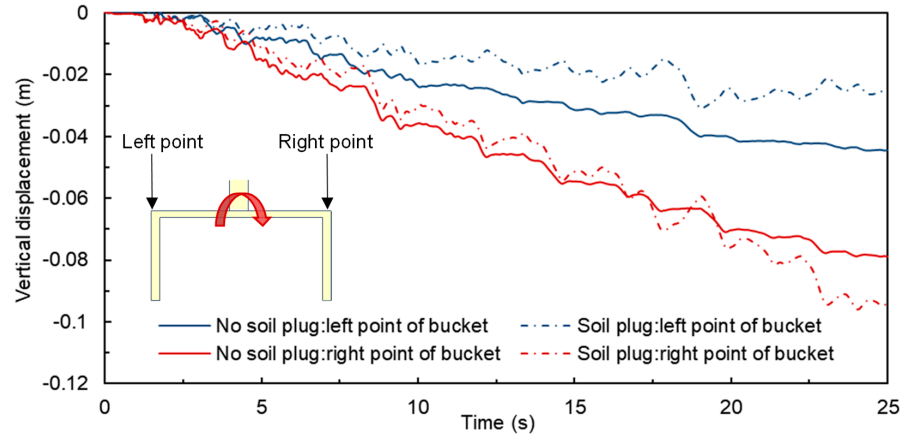


Figure 12. The settlement time histories at the left and right corner points of the wide bucket foundation (WBF) in 50% relative density inclined liquefiable seabeds.

The above analysis is based on a relatively loose (50% relative density) seabed scenario. Similar observations can also be made for a dense seabed with 80% relative density. The maximum horizontal displacement of DBF and WBF in 80% relative density seabed soil are shown in Figure 13a. The maximum horizontal displacement of the bucket foundation in horizontal seabeds increased due to the soil plug, but by a much smaller portion (less than 1%). In inclined ground, the maximum horizontal displacement of the DBF increased by 11.4%, and that of the WBF increased by 15.2% with the presence of soil plug.

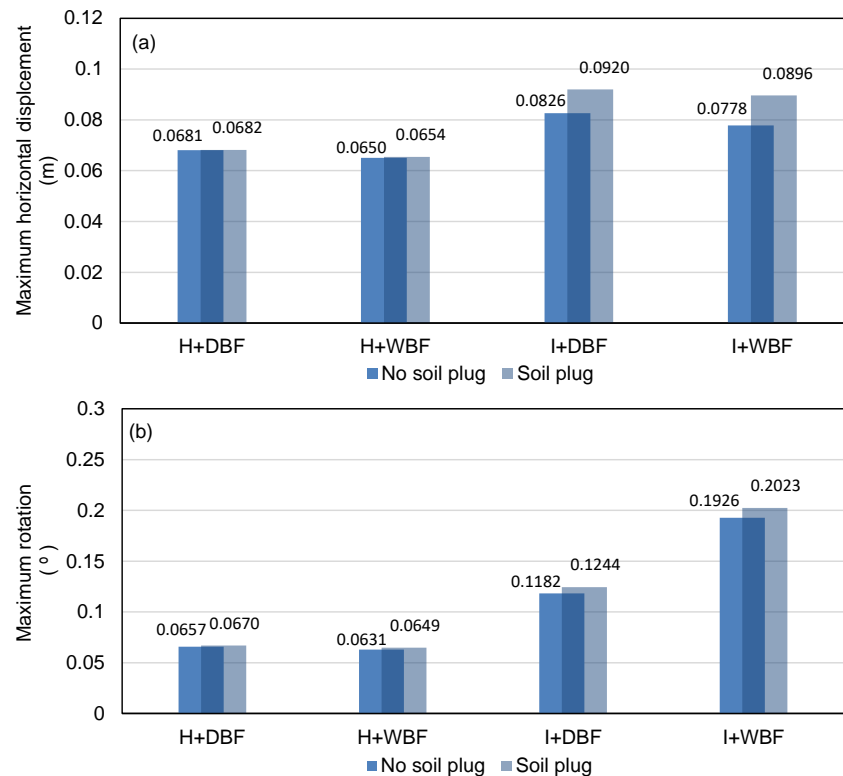


Figure 13. The maximum horizontal displacement and rotation of bucket foundations in 80% relative density liquefiable seabeds: (a) maximum horizontal displacement; (b) maximum rotation.

The maximum rotations of DBF and WBF in 80% relative density seabed soil are shown in Figure 11b. For DBF, the maximum rotation of bucket foundation increased by 2.0% in horizontal ground and by 5.2% in inclined ground due to the presence of soil plug. For WBF, it increased by 2.9% in horizontal ground and by 5.0% in inclined ground. In the dense seabed, the influence of soil plug was less significant compared with in looser seabed.

4. Seismic Response of Bucket Foundation with Different Reinforcement Types

It is clear from the aforementioned analysis that the existence of soil plug has a negative influence on the seismic performance of OWT on bucket foundations in liquefiable seabeds. Therefore, it is important to evaluate the potential improvement in performance when various reinforcement methods are adopted, especially for the more unfavorable inclined seabed conditions. The influence of three reinforcement types for the wide and deep bucket foundations was studied (simulations 6, 8 and 17–28 in Table 4).

According to the time histories of excess pore pressure in seabed soil (Figure 14), the presence of the inner compartment (WBF-C) significantly reduced the excess pore pressure within the bucket foundation, while the reduction of excess pore pressure caused by other reinforcement types were less significant. For near field soil, the presence of the outer wing (WBF-W) reduced the excess pore pressure most significantly. In addition, the soil under the bucket was also reduced, especially by the pile in WBF-P. The reduction in excess pore pressure means that the near field soil would have better resistance to deformation compared with the corresponding case without reinforcement. Similar observations can be made for the deep bucket foundation, and was not repeated for brevity.

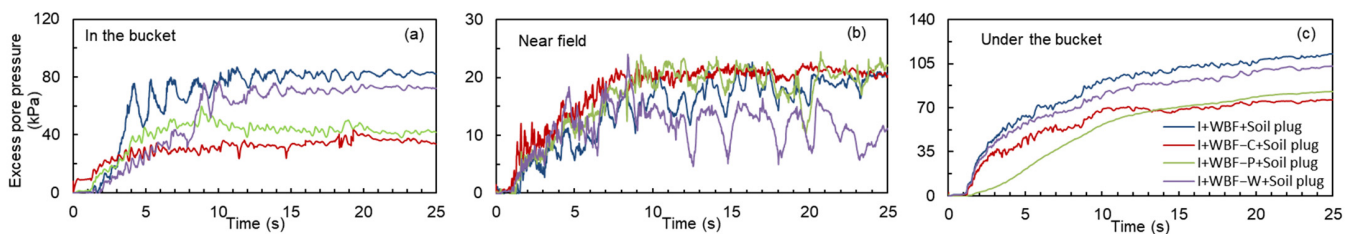


Figure 14. Excess pore pressure time histories of seabed soil near different types of reinforced bucket foundation used in inclined seabeds: (a) seabed soil in the bucket at 2.0 m depth; (b) near field seabed soil at 2.0 m depth; (c) seabed soil under the bucket at 12 m depth.

The effect of different reinforcement types on the displacement and rotation of the bucket foundation was found to be slightly different for deep and wide foundations. For the deep bucket foundation, it was found that the horizontal displacement and the rotation of the bucket foundation was the smallest for DBF-C (Figure 15), especially in terms of rotation, indicating that the reduction in excess pore pressure in soil within the bucket had the greatest influence. The effect of the outer wings and inner pile were unsatisfactory, having marginal influence on limiting the rotation of the bucket. The influence of reinforcement types on maximum bucket displacement and rotation for deep bucket foundation in both horizontal and inclined seabeds are shown in Figure 15c,d. In horizontal seabeds, compared with the case without reinforcement, bucket displacement was reduced by 20.0%, 13.3% and 14.7% for DBF-C, DBF-P and DBF-W, respectively; and bucket rotation was reduced by 48.7%, 13.2% and 14.5% for DBF-C, DBF-P and DBF-W, respectively. In inclined seabed, compared with the case without reinforcement, bucket displacement was reduced by 15.5%, 1.4% and 10.6% for DBF-C, DBF-P and DBF-W, respectively; and bucket rotation was reduced by 70.9%, 7.3% and 10.2% for DBF-C, DBF-P and DBF-W, respectively.

Figure 16 shows the horizontal displacement and rotation of the wide bucket foundation with different reinforcement types. The displacement and rotation of the bucket with inner compartment reinforcement was smallest, which means that the WBF-C is the most effective reinforcement type to improve the seismic performance of wide bucket foundation. However, for the wide bucket foundation, the application of an outer wing and pile can

also significantly reduce the rotation of the bucket. The effect of reinforcement types on maximum bucket displacement and rotation for wide bucket foundations in both horizontal and inclined seabeds are shown in Figure 16c,d. In horizontal seabed, compared with the case without reinforcement, bucket displacement was reduced by 30.3%, 21.1% and 17.1% for DBF-C, DBF-P and DBF-W, respectively; and bucket rotation was reduced by 52.6%, 39.7% and 37.9% for DBF-C, DBF-P and DBF-W, respectively. In inclined seabed, compared with the case without reinforcement, bucket displacement was reduced by 21.9%, 7.5% and 3.4% for DBF-C, DBF-P and DBF-W, respectively; and bucket rotation was reduced by 71.1%, 70.1% and 43.7% for DBF-C, DBF-P and DBF-W, respectively.

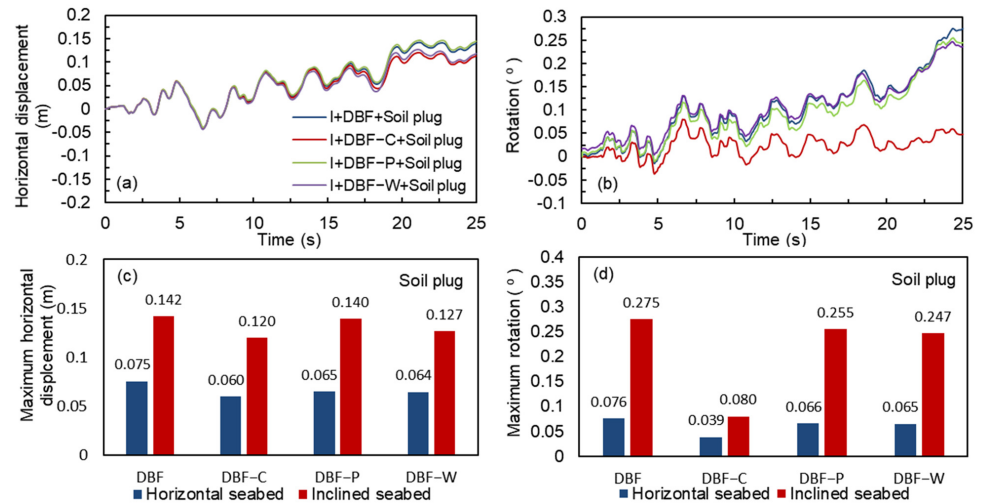


Figure 15. Response of the deep bucket foundation (DBF) with different reinforcement types in 50% relative density inclined liquefiable seabeds: (a) horizontal displacement time histories of deep bucket foundation (DBF) with different reinforcement types; (b) rotation time histories of deep bucket foundation (DBF) with different reinforcement types; (c) The maximum horizontal displacement of deep bucket foundation (DBF) with different reinforcement types; (d) The maximum rotation of deep bucket foundation (DBF) with different reinforcement types.

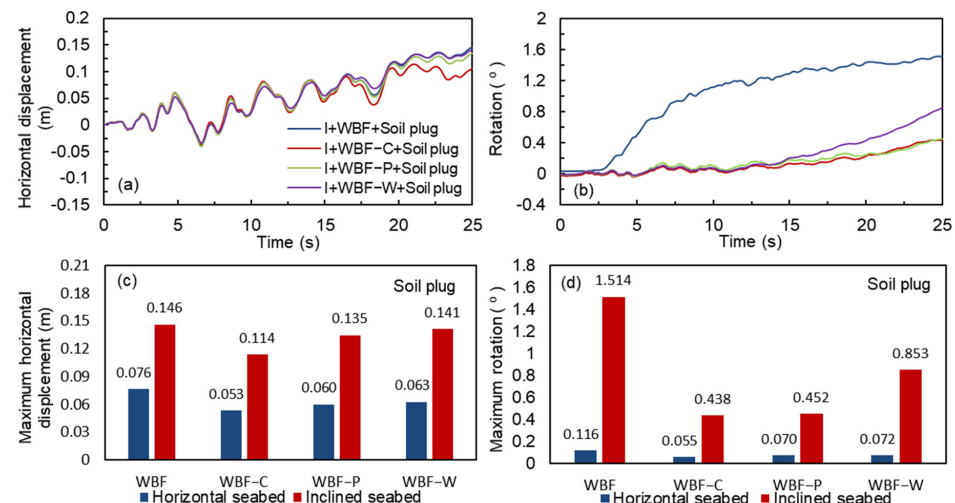


Figure 16. Response of the wide bucket foundation (WBF) with different reinforcement types in inclined seabeds: (a) horizontal displacement time histories of wide bucket foundation (WBF) with different reinforcement types in 50% relative density liquefiable seabeds; (b) rotation time histories of wide bucket foundation (WBF) with different reinforcement types in 50% relative density liquefiable seabeds; (c) the maximum horizontal displacement of wide bucket foundation (WBF) with different reinforcement types in 50% relative density liquefiable seabeds; (d) the maximum rotation of wide bucket foundation (WBF) with different reinforcement types in 50% relative density liquefiable seabeds.

The effect of reinforcement types on maximum wide bucket settlement in inclined seabeds is shown in Figure 17. The nonuniform settlement and maximum settlement of WBF-C was the smallest. The application of outer wings and inner pile can also reduce the nonuniform settlement and right corner point settlement of the bucket to some extent. Compared with the case without reinforcement, the relative settlement of the left and right corners of the bucket was reduced by 72.6%, 42.8% and 29.2% for WBF-C, WBF-P and WBF-W, respectively. The influence of the soil plug and reinforcement methods on bucket settlement was similar to that for the horizontal displacement and rotation.

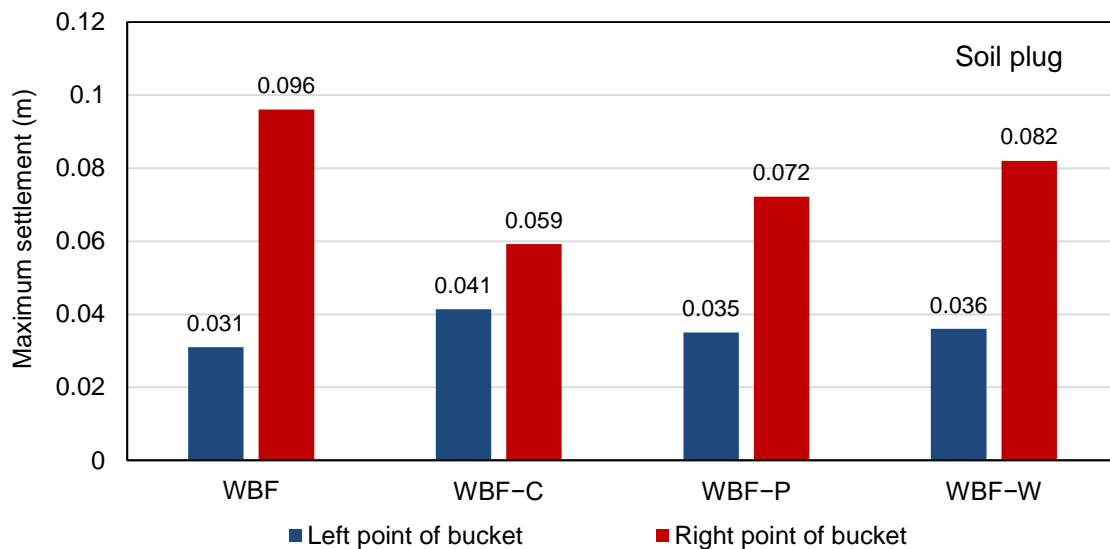


Figure 17. The maximum settlement of the wide bucket foundation (WBF) with different reinforcement types in 50% relative density inclined seabeds.

5. Influence of Soil Plug Removal on Bucket Foundation Response

Several methods to remove soil plug within bucket foundations during installation have recently been proposed. The influence of soil plug removal and a combination of removing the soil plug and using reinforced bucket foundations on seismic response was further analyzed. According to the time histories of excess pore pressure in seabed soil (Figure 18), soil plug removal slightly reduced the excess pore pressure generated in the soil within the bucket for all cases with and without reinforcement. Similar observations were made for the soil under the bucket foundation. This is an indicator that the removal of soil plug can improve the seismic performance of OWT on bucket foundation, even though the reduction in soil density within the bucket due to the generation of the soil plug is not mitigated.

The bucket horizontal displacement time histories of unreinforced and reinforced bucket foundations with soil plug and soil plug removal in inclined seabeds are compared in Figure 19. For unreinforced bucket foundations (DBF or WBF), the horizontal displacement response of the bucket foundation was reduced by removing the soil plug. For the deep bucket foundation, soil plug removal had the greatest influence on the horizontal displacement of DBF-P, while for the wide bucket foundation, soil plug removal had the greatest effect on the horizontal displacement of WBF-W.

In terms of bucket rotation, the removal of soil plug also had a favorable effect (Figure 20). For the deep bucket foundation, the stability of the bucket foundation was slightly improved for the unreinforced and all types of reinforced cases (Figure 20a). For the wide bucket foundation, soil plug removal was shown to massively reduce the rotation of the bucket without reinforcement (Figure 20b). When combined with reinforcement, rotation was further limited by plug removal. Specifically, the rotation of the bucket was brought within the failure rotation criterion of 0.25° when soil plug removal was combined with inner compartment reinforcement (WBF-C).

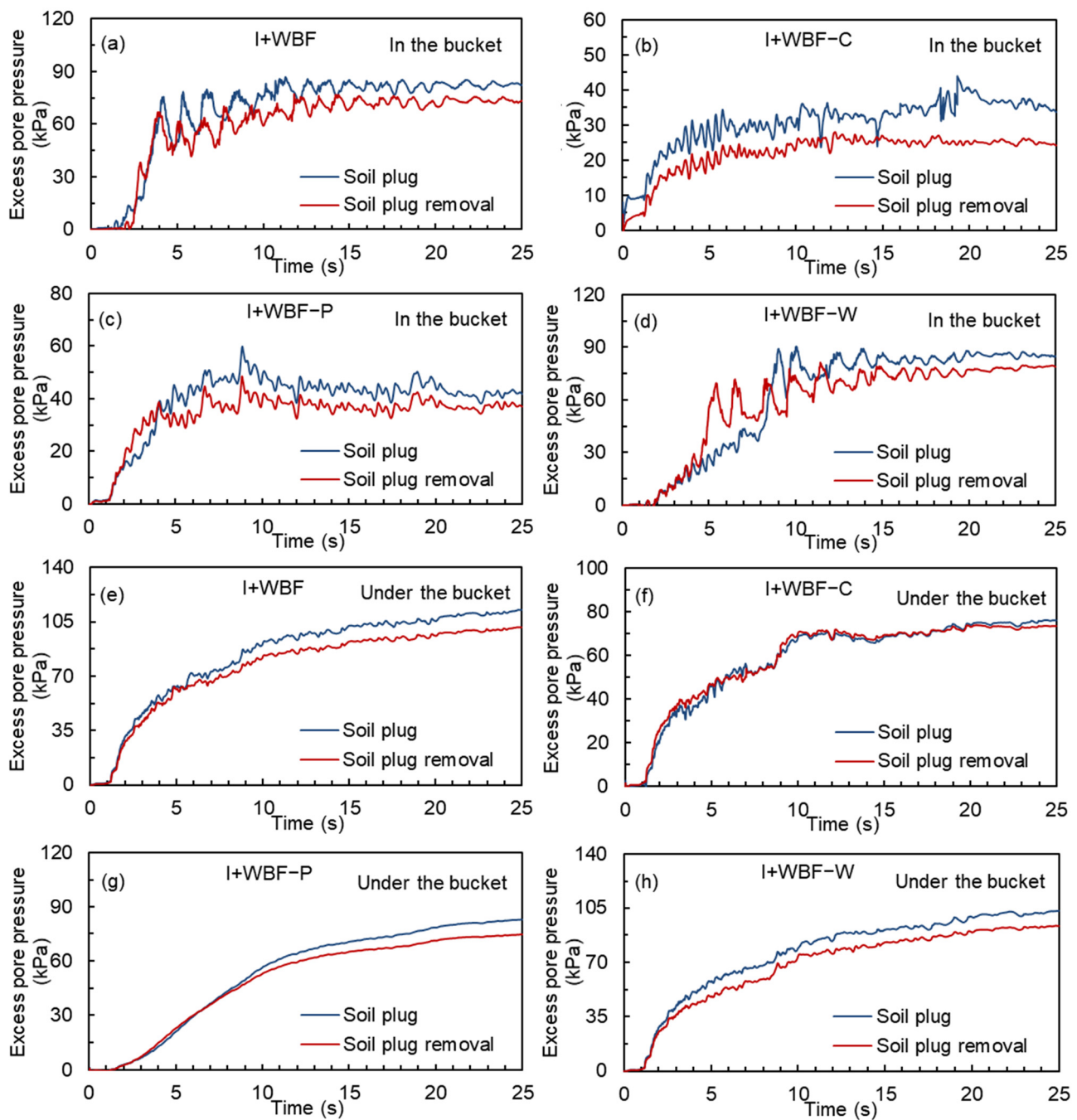


Figure 18. Excess pore pressure time histories of seabed soil for simulations with soil plug and soil plug removal in inclined seabeds: the seabed soil in the bucket (a) WBF; (b) WBF-C; (c) WBF-P; (d) WBF-W; the seabed soil under the bucket: (e) WBF; (f) WBF-C; (g) WBF-P; (h) WBF-W.

The maximum horizontal displacement and rotation for all computed cases in 50% relative density inclined liquefiable seabeds are summarized in Table 5 (simulations 6, 8, 23–28 and 37–44 in Table 4). The presence of soil plug amplified the horizontal displacement of the bucket foundation by 15–25% and the bucket foundation rotation by up to 50–60% for the wide bucket foundation, and should be considered in seismic design. For DBF and WBF, soil plug removal alone (without densification of the inside-bucket soil) can almost eliminate the unfavorable influence of the soil plug on seismic response, indicating that the successful removal and limitation of soil plug during bucket foundation installation is important to the seismic performance of OWT on bucket foundation. In terms of reinforcement, out of the three types of reinforcement types (inner compartment, outer wing and pile within

bucket), the inner compartment was shown to be the most effective in limiting bucket displacement and rotation. By combining inner compartment reinforcement with soil plug removal, the horizontal displacement of the bucket foundation can be reduced by up to 23.3% and the rotation can be reduced by up to 84.7% for the wide bucket foundation in inclined seabeds, compared with the corresponding unreinforced cases with soil plug.

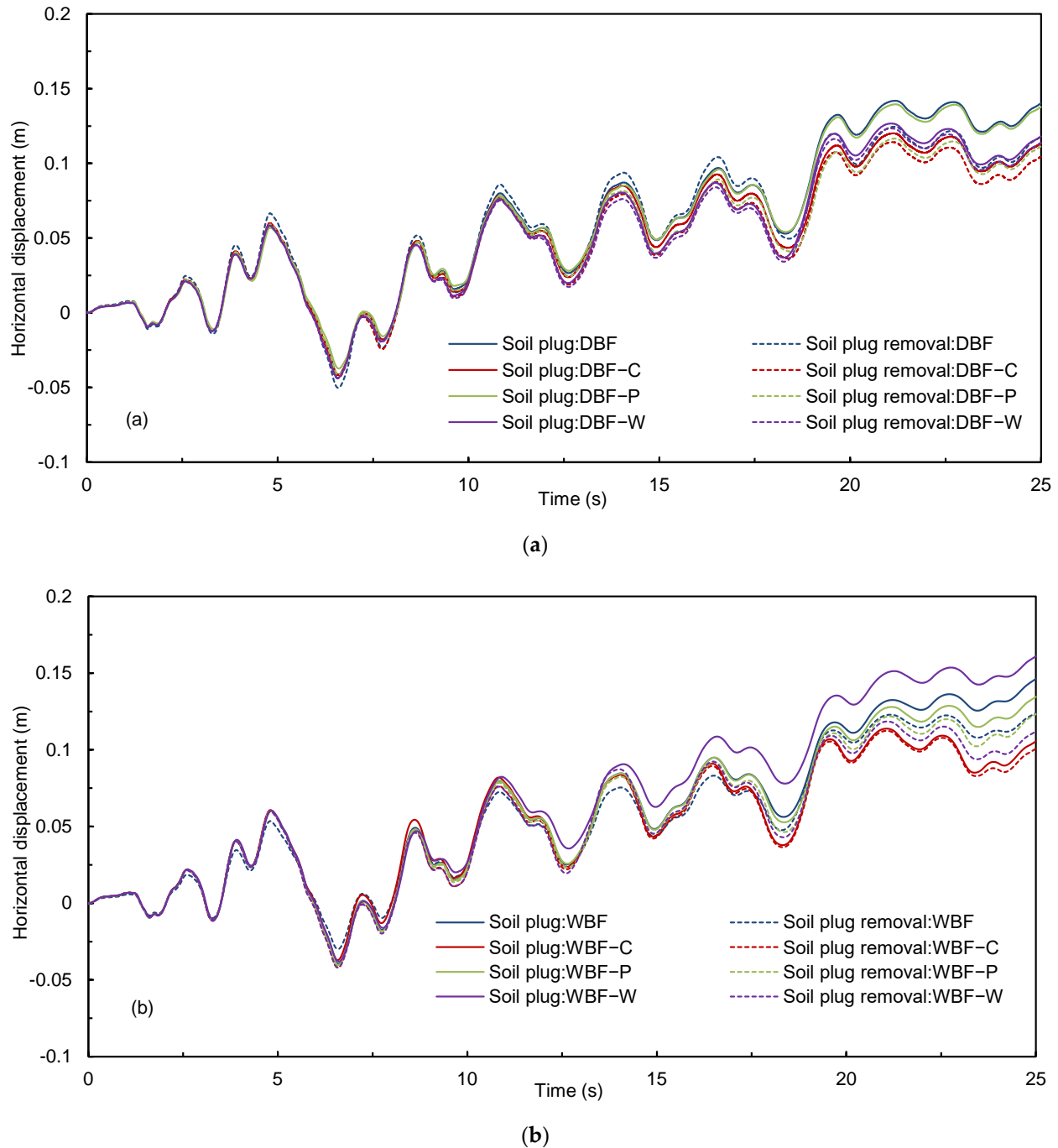
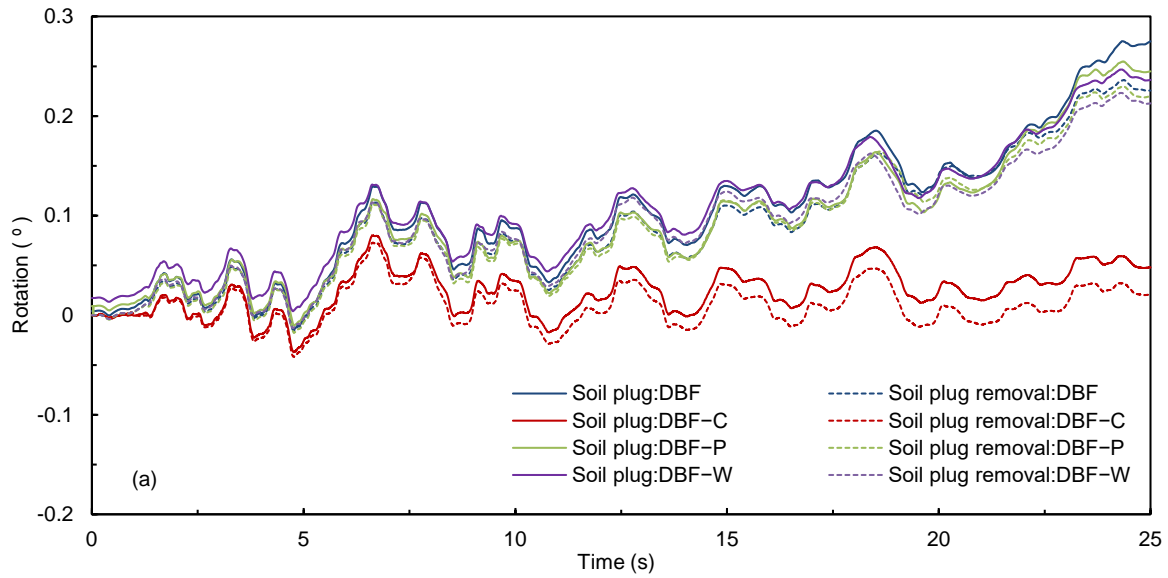
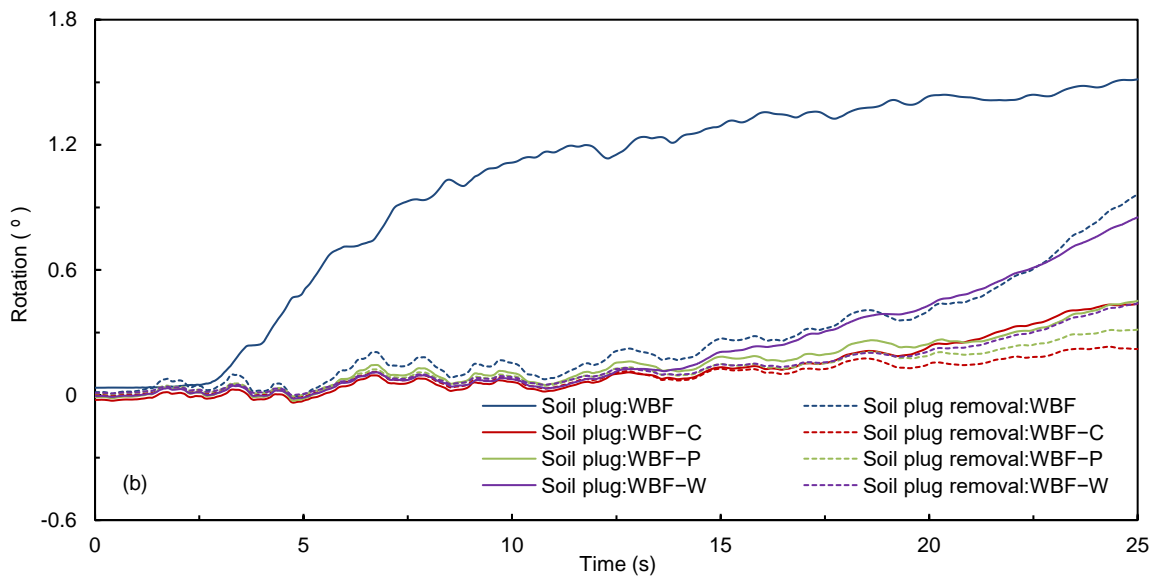


Figure 19. The horizontal displacement time histories of unreinforced and reinforced bucket foundations for simulations with soil plug and soil plug removal in 50% relative density inclined seabeds: (a) deep bucket foundation (DBF); (b) wide bucket foundation (WBF).



(a)



(b)

Figure 20. The rotation time histories of unreinforced and reinforced bucket foundations for simulations with soil plug and soil plug removal in 50% relative density inclined seabeds: (a) deep bucket foundation (DBF); (b) wide bucket foundation (WBF).

Table 5. Influence of different reinforcement types and soil plug removal on maximum horizontal displacement and maximum rotation response of bucket foundation in 50% relative density inclined liquefiable seabeds.

Deep Bucket Foundation		
	Maximum Horizontal Displacement of Bucket Foundation	Maximum Rotation of Bucket Foundation
No soil plug	0.121 (Benchmark)	0.235 (Benchmark)
Influence of soil plug	0.142 (+17.4% compared with no plug)	0.275 (+17.0% compared with no plug)

Table 5. Cont.

Deep Bucket Foundation								
Maximum Horizontal Displacement of Bucket Foundation					Maximum Rotation of Bucket Foundation			
Effect of reinforced types	Unreinforced	Inner-Compartment	Pile–Bucket	Outer-Wings	Unreinforced	Inner-Compartment	Pile–Bucket	Outer-Wings
		0.142	0.120 (−15.5% compared with unreinforced)	0.140 (−1.4% compared with unreinforced)	0.127 (−10.6% compared with unreinforced)	0.275	0.080 (−70.9% compared with unreinforced)	0.255 (−7.3% compared with unreinforced)
Effect of soil plug removal	0.124 (−12.7% compared with no plug removal)	0.114 (−19.7% compared with no plug removal)	0.117 (−17.6% compared with no plug removal)	0.123 (−13.4% compared with no plug removal)	0.236 (−14.2% compared with no plug removal)	0.073 (−73.5% compared with no plug removal)	0.230 (−16.4% compared with no plug removal)	0.223 (−18.9% compared with no plug removal)
Wide Bucket Foundation								
Maximum Horizontal Displacement of Bucket Foundation					Maximum Rotation of Bucket Foundation			
No soil plug	0.119 (Benchmark)				0.951 (Benchmark)			
Influence of soil plug	0.146 (+22.7% compared with no plug)				1.514 (+59.2% compared with no plug)			
Effect of reinforced types	Unreinforced	Inner-Compartment	Pile–Bucket	Outer-Wings	Unreinforced	Inner-Compartment	Pile–Bucket	Outer-Wings
	0.146	0.114 (−21.9% compared with unreinforced)	0.135 (−7.5% compared with unreinforced)	0.141 (−3.4% compared with unreinforced)	1.514	0.438 (−71.1% compared with unreinforced)	0.452 (−70.1% compared with unreinforced)	0.853 (−43.7% compared with unreinforced)
Effect of soil plug removal	0.124 (−15.1% compared with no plug removal)	0.112 (−23.3% compared with no plug removal)	0.123 (−15.8% compared with no plug removal)	0.118 (−19.2% compared with no plug removal)	0.963 (−36.4% compared with no plug removal)	0.232 (−84.7% compared with no plug removal)	0.314 (−79.3% compared with no plug removal)	0.440 (−70.9% compared with no plug removal)

6. Conclusions

In this study, the seismic response of OWT on bucket foundations is studied. The influence of soil plug on the seismic performance of OWT bucket foundations in both horizontal and inclined liquefiable seabeds and the effectiveness of three different reinforcement types and soil plug removal techniques on improving the seismic performance of OWT bucket foundations are evaluated. The main conclusions of this study are as follows:

- (1) The presence of soil plug causes slight amplification of acceleration for the inside-bucket soil, bucket and turbine compared with the case without soil plug. It causes significant increase in the accumulation of excess pore pressure in soil inside and under the bucket, and causes stronger fluctuation in the excess pore pressure of near field soil due to the stronger dynamic interaction between bucket and soil.
- (2) The existence of soil plug has a significant unfavorable influence on the seismic performance of OWT on bucket foundations, especially in inclined liquefiable seabed, resulting in up to a 60% increase in bucket rotation for the wide bucket foundation model, which needs to be considered in the seismic design of OWT. The influence of soil plug is more significant in relatively loose seabed compared with in denser seabed.
- (3) The application of reinforcement methods, including adding an inner compartment, outer wings and inner pile, can improve the seismic performance of OWT on bucket foundation by limiting excess pore pressure generation in near field soil and subsequently reducing bucket displacement, nonuniform settlement and rotation. The application of an inner compartment is found to be the most effective reinforcement type to reduce the seismic response of the bucket.

- (4) Soil plug removal can have a favorable influence on the seismic response of OWT bucket foundation, which can alleviate the undesired influence of the soil plug, and should be adopted when possible. A combination of removing the soil plug and using reinforced bucket foundations can significantly improve the seismic performance of bucket foundation-based OWTs.

It should be pointed out that that the analysis in this study was performed on simple ideal conditions of homogeneous sandy seabed, and this study did not consider the coupled influence of wind and wave loads with seismic load, which could be detrimental once soil liquefaction reaches a considerable depth. The extension of the current findings to more complicated conditions should be treated with care. The comparisons made for the reinforcement methods are based on seismic performance alone, and does not compare construction challenges of the different methods, which should also be considered in practice.

Author Contributions: Conceptualization, R.W.; methodology, R.W. and X.-Q.Q.; investigation, R.W. and X.-Q.Q.; resources, R.W. and B.H.; data curation, X.-Q.Q.; writing—original draft preparation, X.-Q.Q.; writing—review and editing, R.W.; supervision, J.-M.Z. All authors have read and agreed to the published version of the manuscript.

Funding: This research was funded by the National Natural Science Foundation of China, grant number 52022046 and 52038005.

Institutional Review Board Statement: Not applicable.

Informed Consent Statement: Not applicable.

Data Availability Statement: The data presented in this study are available on request from the corresponding author.

Conflicts of Interest: The authors declare no conflict of interest.

References

1. Kaldellis, J.K.; Apostolou, D.; Kapsali, M.; Kondili, E. Environmental and social footprint of offshore wind energy. Comparison with onshore counterpart. *Renew Energy* **2016**, *92*, 543–556. [CrossRef]
2. Simonova, M.D.; Zakharov, V.E. Statistical Analysis of Development Trends in Global Renewable Energy. *Mgimo Rev. Int. Relat.* **2016**, *48*, 214–220. [CrossRef]
3. Swan, S.; Hadjian, A.H. *The 1986 North Palm Springs Earthquake: Effects on Power Facilities*; No. EPRI-NP-5607; EQE, Inc.: San Francisco, CA, USA; Bechtel Power Corp.: Norwalk, CA, USA, 1988.
4. Prowell, I.; Veers, P. Assessment of Wind Turbine Seismic Risk: Existing Literature and Simple Study of Tower Moment Demand. Sandia National Laboratories (SNL), Albuquerque, NM, and Livermore, CA (United States). 2009. Available online: <https://www.osti.gov/biblio/983699> (accessed on 7 February 2023). [CrossRef]
5. Butt, U.A.; Ishihara, T. Seismic Load Evaluation of Wind Turbine Support Structures Considering Low Structural Damping and Soil Structure Interaction. *Eur. Wind. Energy Assoc. Annu. Event* **2012**, *4*, 16–19.
6. Ritschel, U.; Warnke, I.; Kirchner, J.; Meussen, B. Wind turbines and earthquakes. In Proceedings of the 2nd World Wind Energy Conference, Cape Town, South Africa, 24 November 2003.
7. Asareh, M.A.; Schonberg, W.; Volz, J. Effects of seismic and aerodynamic load interaction on structural dynamic response of multi-megawatt utility scale horizontal axis wind turbines. *Renew Energy* **2016**, *86*, 49–58. [CrossRef]
8. Risi, R.D.; Bhattacharya, S.; Goda, K. Seismic performance assessment of monopile-supported offshore wind turbines using unscaled natural earthquake records. *Soil Dyn. Earthq. Eng.* **2018**, *109*, 154–172. [CrossRef]
9. Kaynia, A.M. Seismic considerations in design of offshore wind turbines. *Soil Dyn. Earthq. Eng.* **2019**, *124*, 399–407. [CrossRef]
10. Cui, C.Y.; Meng, K.; Wu, Y.J.; Chapman, D.; Liang, Z.M. Dynamic response of pipe pile embedded in layered visco-elastic media with radial inhomogeneity under vertical excitation. *Geomech. Eng.* **2018**, *16*, 609–618.
11. Cui, C.Y.; Liang, Z.M.; Xu, C.S.; Xin, Y.; Wang, B.L. Analytical solution for horizontal vibration of end-bearing single pile in radially heterogeneous saturated soil. *Appl. Math. Model.* **2023**, *116*, 65–83. [CrossRef]
12. Meng, K.; Cui, C.Y.; Liang, Z.M.; Li, H.J.; Pei, H.F. A new approach for longitudinal vibration of a large-diameter floating pipe pile in visco-elastic soil considering the three-dimensional wave effects. *Comput. Geotech.* **2020**, *128*, 103840. [CrossRef]
13. Gao, B.; Zhu, W.X.; Zhang, Q.; Ye, G.L. Response of suction bucket foundation subjected to wind and earthquake loads on liquefiable sandy seabed. *Soil Dyn. Earthq. Eng.* **2022**, *160*, 107338. [CrossRef]

14. Wen, F. Developments and characteristics of offshore wind farms in China. *Adv. New Renew. Energy* **2016**, *4*, 152–158.
15. Shang, W.M. Study on engineering geological conditions of Xinghua Bay offshore wind farm in Fuqing. *Low Carbon World* **2017**, *22*, 61–62.
16. Qu, X.Q.; Zhang, Z.T.; Hu, J.; Wang, R.; Zhang, J.M. Centrifuge shaking table tests on offshore wind turbine bucket foundation in mildly inclined liquefiable seabed. *Soil Dyn. Earthq. Eng.* **2021**, *151*, 107012. [[CrossRef](#)]
17. Senpere, D.; Auvergne, G.A. Suction anchor piles—a proven alternative to driving or drilling. In Proceedings of the Offshore Technology Conference, Houston, TX, USA, 3–6 May 1982.
18. Tjelta, T.I. Geotechnical experience from the installation of the Europipe jacket with bucket foundations. In Proceedings of the Offshore Technology Conference, Houston, TX, USA, 1–4 May 1995.
19. Allersma, H.G.B.; Plenevaux, F.J.A.; Wintgens, J.F. Simulation of suction pile installation in sand in a geocentrifuge. In Proceedings of the Seventh International Offshore and Polar Engineering Conference, Honolulu, HI, USA, 1 January 1997.
20. Ding, H.Y.; Liu, Z.Y.; Chen, X. Model tests on soil plug formation in suction anchor for silty clay. *J. Geotech. Eng.* **2001**, *169*, 214–223.
21. Tran, M.N.; Randolph, M.F.; Airey, D.W. Installation of suction caissons in sand with silt layers. *J. Geotech. Geoenviron. Eng.* **2007**, *133*, 1183–1191. [[CrossRef](#)]
22. Wang, H. Research on Penetration Resistance and Uplift Bearing Capacity Evolution of Suction Caisson and Soil Plug Removal. Ph.D. Thesis, Tsinghua University, Beijing, China, 2022.
23. Yu, H.; Zeng, X.W.; Lian, J.J. Seismic behavior of offshore wind turbine with suction caisson foundation. In Proceedings of the 2014 Geo-Congress, Atlanta, Georgia, 23–26 February 2014.
24. Wang, X.F.; Zeng, X.W.; Yu, H.; Wang, H.J. Centrifuge modeling of offshore wind turbine with bucket foundation under earthquake loading. In Proceedings of the International Foundations Congress and Equipment Expo (IFCEE) 2015, San Antonio, Texas, 17–21 March 2015.
25. Olalo, L.T.; Choo, Y.W.; Bae, K.T. Influence of the Skirt on the Seismic Response of Bucket Foundations for Offshore Wind Tower Using Dynamic Centrifuge Model Tests. In Proceedings of the ASME 2016 35th International Conference on Ocean, Offshore and Arctic Engineering, Busan, Republic of Korea, 19–24 June 2016.
26. Wang, R.; Liu, X.; Zhang, J.M. Numerical analysis of the seismic inertial and kinematic effects on pile bending moment in liquefiable soils. *Acta Geotech.* **2017**, *12*, 773–791. [[CrossRef](#)]
27. Wang, X.F.; Zeng, X.W.; Yang, X.; Li, J.L. Seismic response of offshore wind turbine with hybrid monopile foundation based on centrifuge modelling. *Appl. Energy* **2019**, *235*, 1335–1350. [[CrossRef](#)]
28. Li, X.Y.; Zeng, X.W.; Yu, X.; Wang, X.F. Seismic response of a novel hybrid foundation for offshore wind turbine by geotechnical centrifuge modeling. *Renew Energy* **2021**, *172*, 1404–1416. [[CrossRef](#)]
29. Zayed, M. Experimental and Numerical Seismic Response of Offshore Wind Turbines Supported on Bucket Foundations. Ph.D. Dissertation, University Of California San Diego, San Diego, CA, USA, 2022.
30. Asheghabadi, M.S.; Jebeli, A.J. Seismic Behavior of Suction Caisson Foundations. *Int. J. Geotech. Geol. Eng.* **2019**, *13*, 30–36.
31. Gao, B.; Ye, G.L.; Zhang, Q.; Xie, Y.; Yan, B. Numerical simulation of suction bucket foundation response located in liquefiable sand under earthquakes. *Ocean Eng.* **2021**, *235*, 109394. [[CrossRef](#)]
32. Wang, X.F.; Ma, C.L.; Li, J.L. Seismic response of suction bucket foundation for offshore wind turbines: A parametric study. *Ocean Eng.* **2022**, *257*, 111570. [[CrossRef](#)]
33. Esfeh, P.K.; Kaynia, A.M. Earthquake response of monopiles and caissons for Offshore Wind Turbines founded in liquefiable soil. *Soil Dyn. Earthq. Eng.* **2020**, *136*, 106213. [[CrossRef](#)]
34. Ueda, K.; Uzuoka, R.; Iai, S.; Okamura, T. Centrifuge model tests and effective stress analyses of offshore wind turbine systems with a suction bucket foundation subject to seismic load. *Soils Found.* **2020**, *60*, 1546–1569. [[CrossRef](#)]
35. Kourkoulis, R.S.; Lekakakis, P.C.; Gelagoti, F.M.; Kaynia, A.M. Suction caisson foundations for offshore wind turbines subjected to wave and earthquake loading: Effect of soil-foundation interface. *Geotechnique* **2014**, *64*, 171–185. [[CrossRef](#)]
36. Zhang, P.Y.; Xiong, K.P.; Ding, H.Y.; Le, C.H. Anti-liquefaction characteristics of composite bucket foundations for offshore wind turbines. *J. Renew Sustain. Energy* **2014**, *6*, 053102. [[CrossRef](#)]
37. Eslami, A.; Ghorbani, A. Seismic response of offshore wind turbines supported on Monopiles and Suction Buckets: Numerical modelling and soft computing study. *Soil Dyn. Earthq. Eng.* **2022**, *159*, 107284. [[CrossRef](#)]
38. Liu, H.; Wu, W.B.; Jiang, G.S.; El Naggar, M.H.; Mei, G.X.; Liang, R.Z. Influence of soil plug effect on the vertical dynamic response of large diameter pipe piles. *Ocean Eng.* **2018**, *157*, 13–25. [[CrossRef](#)]
39. Lehane, B.; Powrie, W.; Doherty, J. Centrifuge model tests on piled footings in clay for offshore wind turbines. In Proceedings of the Second International Symposium on Frontiers in offshore Geotechnics (ISFOG), University of Western Australia, Perth, Australia, 8–10 November 2010.
40. Li, D.Y.; Zhang, Y.K.; Feng, L.Y.; Gao, Y.F. Capacity of modified suction caissons in marine sand under static horizontal loading. *Ocean Eng.* **2015**, *102*, 1–16. [[CrossRef](#)]
41. Wang, X.F.; Yang, X.; Zeng, X.W. Seismic centrifuge modelling of suction bucket foundation for offshore wind turbine. *Renew Energy* **2017**, *114*, 1013–1022. [[CrossRef](#)]

42. Faizi, K.; Faramarzi, A.; Dirar, S.; Chapman, D. *Finite Element Modelling of the Performance of Hybrid Foundation Systems for Offshore Wind Turbines*; Springer: Berlin/Heidelberg, Germany, 2019.
43. Zhang, P.Y.; Li, J.Y.; Le, C.H.; Ding, H.Y. Seismic responses of two bucket foundations for offshore wind turbines based on shaking table tests. *Renew Energy* **2022**, *187*, 1100–1117. [[CrossRef](#)]
44. Chen, W.Y.; Jiang, Y.J.; Xu, L.Y.; Liu, C.; Chen, G.X.; Wang, P.G. Seismic response of hybrid pile-bucket foundation supported offshore wind turbines located in liquefiable soils. *Ocean Eng.* **2023**, *269*, 113519. [[CrossRef](#)]
45. Dimmock, P.; Clukey, E.; Randolph, M.F.; Murff, D.; Gaudin, C. Hybrid Subsea Foundations for Subsea Equipment. *J. Geotech. Geoenviron. Eng.* **2013**, *139*, 2182–2192. [[CrossRef](#)]
46. Fu, D.F.; Bienen, B.; Gaudin, C.; Cassidy, M. Undrained capacity of a hybrid subsea skirted mat with caissons under combined loading. *Can. Geotech. J.* **2014**, *51*, 934–949. [[CrossRef](#)]
47. Kim, J.H.; Kim, S.; Kim, D.S. Bearing capacity of hybrid suction foundation on sand with loading direction via centrifuge model test. *Jpn. Geotech. Soc. Spec. Publ.* **2016**, *2*, 1339–1342. [[CrossRef](#)]
48. Chen, X.G.; Ma, Q.S.; Jiang, Y.K.; Xu, J.P. A offshore wind turbine suction bucket foundation for soil plug removal. Shandong province, China. CN105926661A, 7 September 2016.
49. An, J.B.; Liu, J.L.; Wang, C.H.; LIU, J.Q. A bucket foundation capable of reducing soil plug. Anhui province, China. CN109306705B, 27 November 2020.
50. He, B.; Shen, K.M.; Qi, H.F. A sub-cabin bucket foundation with anti-soil plug and reverse grouting. Zhejiang province, China. CN213390204U, 8 June 2021.
51. Itasca Consulting Group Inc. Fast Language Analysis of Continua in 3 Dimensions, Version 5.0, User's manual. Minneapolis, Minnesota. 2012. Available online: <https://www.itascacg.com/software/flac3d> (accessed on 7 February 2023).
52. Qu, X.Q.; Wang, R.; Zhang, J.M. Centrifuge and Numerical Simulation of Offshore Wind Turbine Suction Bucket Foundation Seismic Response in Inclined Liquefiable seabed. In *Conference on Performance-Based Design in Earthquake. Geotechnical Engineering*; Springer: Berlin/Heidelberg, Germany, 2022; pp. 1215–1221.
53. Wang, R.; Zhang, J.M.; Wang, G. A unified plasticity model for large post-liquefaction shear deformation of sand. *Comput. Geotech.* **2014**, *59*, 54–66. [[CrossRef](#)]
54. Zou, Y.X.; Zhang, J.M.; Wang, R. Seismic analysis of stone column improved liquefiable seabed using a plasticity model for coarse-grained soil. *Comput. Geotech.* **2020**, *125*, 103690. [[CrossRef](#)]
55. He, B.; Zhang, J.M.; Li, W.; Wang, R. Numerical analysis of LEAP centrifuge tests on sloping liquefiable seabed: Influence of dilatancy and post-liquefaction shear deformation. *Soil Dyn. Earthquake Eng.* **2020**, *137*, 106288. [[CrossRef](#)]
56. Liu, H.X.; Zhang, J.M.; Zhang, X.D.; Wang, R. Seismic performance of block-type quay walls with liquefiable calcareous sand backfill. *Soil Dyn. Earthq. Eng.* **2020**, *132*, 106092. [[CrossRef](#)]
57. Zhu, T.; Wang, R.; Zhang, J.M. Evaluation of various seismic response analysis methods for underground structures in saturated sand. *Tunn. Undergr. Space Technol.* **2021**, *110*, 103803. [[CrossRef](#)]
58. Li, Y.Y.; Luo, C.; Zhang, J.M.; Liu, F.; Wang, R. Rayleigh Wave-Shear Wave Coupling Mechanism for Large Lateral Deformation in Level Liquefiable seabed. *Comput. Geotech.* **2022**, *143*, 104631. [[CrossRef](#)]
59. Wang, R. Influence of vertical ground motion on the seismic response of underground structures and underground-aboveground structure systems in liquefiable seabed. *Tunn. Undergr. Space Technol.* **2022**, *122*, 104351. [[CrossRef](#)]
60. Li, Y.Y.; Wang, R.; Zhang, J.M. A stepwise artificial boundary condition for wave propagation in elasto-plastic media. *Soil Dyn. Earthq. Eng.* **2023**, *165*, 107733. [[CrossRef](#)]
61. Yang, S.L.; Li, A.L.; Qi, J.F. Experimental study on bucket foundation during penetration by suction. *J. Geotech. Eng.* **2003**, *14*, 236–238.
62. Guo, Z.; Jeng, D.S.; Guo, W.; He, R. Simplified approximation for seepage effect on penetration resistance of suction caissons in sand. *Ships Offshore Struct.* **2017**, *12*, 980–990. [[CrossRef](#)]
63. Tran, M.N. Installation of suction caissons in dense sand and the influence of silt and cemented layers. Ph.D. Thesis, School of Civil Engineering, University of Sydney, Sydney, Australia, 2005.
64. Liu, X. Research on Seismic Response of Pile Group in Liquefiable Ground. Ph.D. Thesis, Tsinghua University, Beijing, China, 2018.
65. Du, J.; Ding, H.Y.; Liu, J.H.; Zhang, C. Research on boundary selection of soil of bucket foundation with finite element analysis. *Ocean Technol.* **2005**, *24*, 109–113.
66. Yang, M.; Luo, R.P.; Li, W.C. Numerical study on accumulated deformation of laterally loaded monopiles used by offshore wind turbine. *Bull. Eng. Geol. Environ.* **2018**, *77*, 911–921. [[CrossRef](#)]
67. Chaloulos, Y.K.; Tsiapas, Y.Z.; Bouckovalas, G.D. Seismic analysis of a model tension leg supported wind turbine under seabed liquefaction. *Ocean Eng.* **2021**, *238*, 109706. [[CrossRef](#)]
68. GB 17741-2005; Evaluation of Seismic Safety for Engineering Sites. Standards Press of China: Beijing, China, 2005.
69. GB50011-2010; Code for Seismic Design of Buildings. Architecture & Building Press: Beijing, China, 2010.
70. GB 18306-2015; Seismic Ground Motion Parameter Zonation Map of China. Standards Press of China: Beijing, China, 2015.

71. Hesar, M. Geotechnical design of the Barracuda and Caratinga suction anchors. In Proceedings of the Offshore Technology Conference, Houston, TX, USA, 5–8 May 2003.
72. Peire, K.; Nonneman, H.; Bosschem, E. Gravity base foundations for the Thornton bank offshore wind farm. *Terraet Aqua*. **2009**, *115*, 19–29.

Disclaimer/Publisher's Note: The statements, opinions and data contained in all publications are solely those of the individual author(s) and contributor(s) and not of MDPI and/or the editor(s). MDPI and/or the editor(s) disclaim responsibility for any injury to people or property resulting from any ideas, methods, instructions or products referred to in the content.